THE ASTROPHYSICAL JOURNAL, 324:501–515, 1988 January 1

MOLECULAR HYDROGEN MAPS OF EXTENDED PLANETARY NEBULAE: THE DUMBBELL, THE RING, AND NGC 2346

B. ZUCKERMAN
University of California, Los Angeles

AND

IAN GATLEY
National Optical Astronomy Observatories
Received 1987 January 8; accepted 1987 June 22

ABSTRACT

We have detected and mapped 2 μm H_2 emission toward three famous planetary nebulae (PN). In the Dumbbell (NGC 6853) and the Ring (NGC 6720) the H_2 emission is very extensive and lies outside, but otherwise closely traces, the main distribution of ionized gas. In NGC 2346 the H_2 emission also follows the distribution of ionized gas; in addition there is evidence for a dense torus of neutral gas that surrounds the central star and lies in a direction perpendicular to that of the optical bipolar lobes. The H_2 emission appears to be shock-excited. We considered shocks driven into molecular clouds by the pressure of the expansion of ionized gas and also by fast stellar winds in both uniform and clumpy models. When we assumed that the $v = 1$ level of H_2 is excited by collisions with other H_2 molecules, in no case were we able to find a plausible force to drive a shock that could match the observed intensity of $S(1)$ emission. Vibrational excitation rates due to collisions of H with H_2 are very uncertain, but this type of collision could explain our observations if a modest percentage of the hydrogen is in atomic form in the shocked layers.

We examined existing H_2 measurements of PN and conclude that strong H_2 emission is preferentially present in PN that lie at small galactic latitude. The implication is that massive main-sequence stars produce ionization-bounded PN, whereas low-mass stars produce density-bounded PN during most of the observable lifetimes of the PN. This is consistent with time-dependent models of PN evolution described by Giuliani. In particular, the time rate of change of the ionizing luminosity of the central star is critical in determining whether a given PN will be ionization-bounded or density-bounded. Maps of H_2 emission may, therefore, be used not only to determine whether a given PN is ionization-bounded, but also to estimate the mass of the progenitor star.

We find that "bow tie"–like PN display H_2 emission; this is consistent with predictions of morphological models for this class of PN. More generally, since bow tie nebulae appear to be concentrated toward the galactic plane, this particular PN morphology is apparently associated with massive progenitor stars and is unlikely to be the result of the gravitational field of a close companion star as has been suggested in some morphological models. The case for stellar rotation as the agent responsible for the bow tie morphology is also very weak in spite of the fact that rotation is rapid in massive main-sequence stars. In any event, neither close companion stars nor rotation of the red giant progenitor of the PN can plausibly explain the full range of bipolar and elliptical symmetries observed in PN.

Radio molecular and infrared continuum data imply that many, probably most, and possibly all, post–asymptotic giant branch (AGB) stars terminate rapid mass loss while the star still has a fairly low effective temperature ($T_{\rm eff}$). Therefore, evolutionary tracks for post–AGB stars that assume continued rapid mass loss when $T_{\rm eff} \gtrsim 10^4$ K are unlikely to be correct. If the standard evolutionary tracks for post–AGB stars that run at constant luminosity to large $T_{\rm eff}$ ($\gtrsim 10^5$ K) are correct, then the termination of rapid mass loss must be due to cessation of stellar pulsations and/or small dust-to-gas ratios in the circumstellar material.

Subject headings: interstellar: molecules — nebulae: planetary

I. INTRODUCTION

Two fundamental unsolved problems in our understanding of planetary nebulae (PN) are their distances from Earth and the physical mechanism that ejects and shapes the outflowing ionized gas cloud. Conventional methods for obtaining distances to individual PN usually require knowledge of whether the PN is ionization-bounded or density-bounded (see, e.g., Kaler 1985 and Kwok 1985 and references therein). Oftentimes even this minimal knowledge is uncertain or simply not available from optical spectra. According to conventional morphological models, which we discuss in some detail in § V*b*, a given bipolar PN could reasonably be expected to be partially ionization-bounded and partially density-bounded. Since approximately 50% of all PN are bipolar (Zuckerman and Aller 1986, hereafter ZA), a determination of the distribution of neutral gas, if any, over the entire faces of these PN is critical in an evaluation of these models. Determination of Zanstra temperatures for the central stars also requires knowledge of whether the PN is ionization-bounded.

A direct method to determine if a given PN is ionization-bounded is to detect a substantial surrounding molecular cloud, i.e., the un-ionized remnant of the wind from the progenitor red giant star. Millimeter wave searches for CO have been largely fruitless (e.g., Knapp 1985 and references therein),

although recent observations by Huggins and Healy (1986*a*, *b*) have somewhat improved the detection rate. Near-infrared searches for H_2 emission have been more successful (e.g., Storey 1984 and references therein). However, even these searches have been spotty and include only a few maps of individual PN. In particular, according to Storey, "there is no clear correlation between H_2 emission and any other characteristic of the source. This is emphasized by the widely differing nature of the sources in which H_2 is detected."

In an attempt to improve this unsatisfactory situation, we have used a system having a large field of view and high spectral resolution on a large telescope to obtain complete H_2 maps of three extended PN that are representative of two of the most common PN morphologies—bow tie and bipolar ring. We also searched for H_2 in a few additional PN. An examination of all H_2 data that are known to us has revealed a number of striking correlations that relate to the ejection mechanism for and evolution of PN. We describe the observational procedures in § II. Section III is a very brief review (tutorial) on aspects of PN that are relevant to analysis of our H_2 maps which are discussed in § IV. Section V is a discussion of shock excitation of and morphological and evolutionary models for PN.

II. OBSERVATIONS

Almost all the data were obtained with the 3.8 m United Kingdom Infrared Telescope (UKIRT) at Mauna Kea, Hawaii, in 1985 May, July, October, and December and 1986 October. The map of the Dumbbell nebula (Fig. 1) was obtained by locking a Fabry-Perot spectrometer (resolution, $\lambda/\Delta\lambda \approx 2300$) to the wavelength (2.122 μm) of the $v = 1 \rightarrow 0$ $S(1)$ line of H_2 and subtracting the energy received at a position 12′ off the PN from the energy received on the PN. Because this "total power" technique is sensitive to continuum radiation from field stars that happen to be in some "on" or "off" positions, we obtained a spectrum at each of the apparent peaks in the H_2 map. Spectra without clear H_2 emission implied the presence of a contaminating star in the total power map. In each such case, we interpolated the H_2 contour levels from adjacent map positions across the position of the star. The total time spent per pixel in the map was 40 s, 20 s of which were spent on the Dumbbell nebula. We also obtained some spectra with a circular variable filter ("CVF," $\lambda/\Delta\lambda \approx 117$) that covered both the $S(1)$ line and hydrogen Brackett-γ (2.166 μm). The relative strength of the $S(1)$ and Brγ emission indicated that the fluxes measured toward the Dumbbell with the Fabry-Perot were not due to nebular free-free continuum emission.

The map of the Ring nebula (Fig. 2) was obtained with the Fabry-Perot using a standard beam-switching technique. A chopping secondary mirror defined primary and reference positions 2′ apart in the east-west direction. Integrations were alternated with the nebula placed in one beam and then in the other while chopping to an off-source position at 3.5 Hz. The total time spent per pixel in the map was 8 s, 4 s of which were

FIG. 1.—H_2 map of the $S(1)$, $v = 1 \rightarrow 0$, line from NGC 6853 overlaid on a photograph obtained by Dr. L. Thompson and Mr. M. Pierce on the 3.6 m Canada-France-Hawaii Telescope using hypersensitized color film. (See cover of 1983 July issue of *Sky and Telescope* for the original color photograph.) The beam diameter for the H_2 map was 19″.6, and the map points were separated by 40″. Because of this coarse sampling interval, the reality of small-scale features, in particular the $S(1)$ emission peak at the central star, should be regarded with caution. The $S(1)$ contours are logarithmically spaced. The peak contour corresponds to 7.5×10^{-20} W cm^{-2} in a 19″.6 beam, and the ratio between contours is a factor of 1.41. The rectangle that encloses the $S(1)$ contours is 480″ (NS) by 640″ (EW) with north toward its top and east toward the left. $S(1)$ emission was searched for over the entire area of the rectangle.

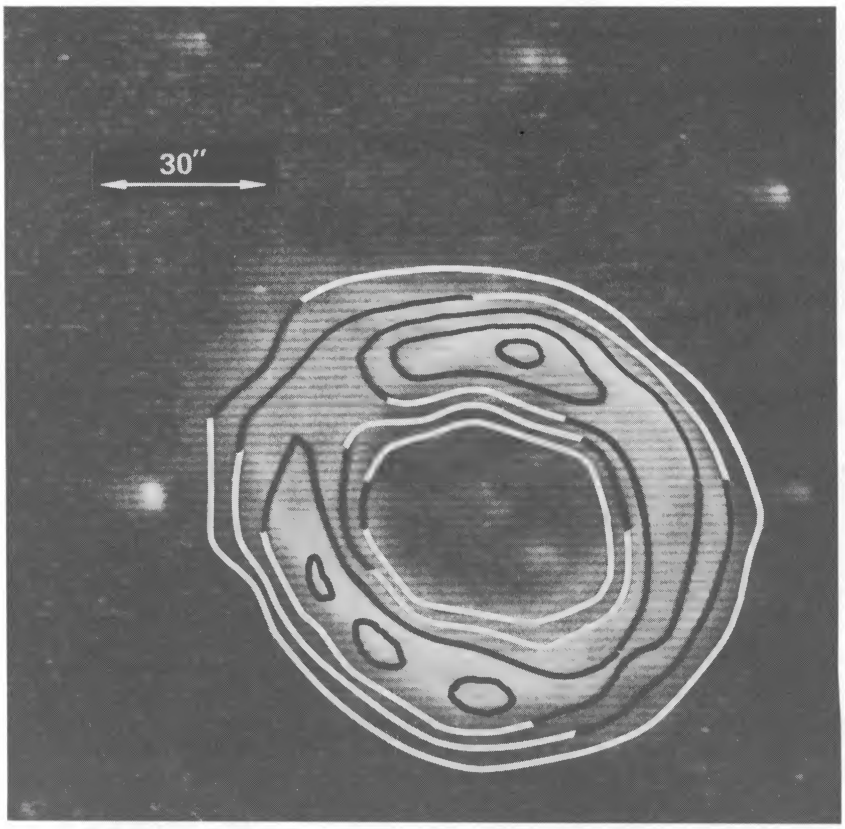

FIG. 2.—$S(1)$ $v = 1 \rightarrow 0$ contour map on an [O I] λ6300 picture of NGC 6720 obtained by Dr. B. Balick with the 2.1 m telescope and CCD camera at Kitt Peak National Observatory. The [O I] contrast has been altered intentionally so as to bring up faint features while preserving the highlights. The [O I] data were obtained under conditions of excellent transparency and approximately 1″ seeing. The beam diameter for the $S(1)$ map was 19.″6, and the map points were separated by 10″. The contours are linearly spaced. The peak contour corresponds to 9×10^{-20} W cm^{-2} in a 19.″6 beam and the spacing between contours is 1.3×10^{-20} W cm^{-2}. Given the 19.6 beam diameter, apparent positional discrepancies between optical and $S(1)$ features that are $\lesssim$10″ should not be trusted. North is toward the top, and east is toward the left.

spent on the Ring nebula. As Beckwith, Persson, and Gatley (1978) showed and we confirm (Table 2), the distribution of $S(1)$ emission is significantly different from that of the ionized gas. In particular, the contribution of nebular continuum emission to all points in the map in Figure 2 is negligible ($\lesssim$1%).

The map of NGC 2346 (Fig. 3) was obtained by switching the Fabry-Perot at a rate 1 Hz, between the $S(1)$ frequency and an "off" frequency, 220 km s^{-1} lower, that appeared to be free of significant spectral emission. This technique discriminates against all energy sources that are constant over tiny spectral ranges (e.g., stars, nebular free-free emission, etc.), but it is sensitive to weak spectral features other than the $S(1)$ line from either NGC 2346 or the atmosphere of Earth at both the $S(1)$ and the off frequencies. The integration time was 8 s per map pixel.

The fluxes and upper limits listed in Table 3A were obtained using methods similar to those described above.

Figure 4 displays CVF spectra of the so-called K window obtained at positions of peak $S(1)$ emission in the Ring, the Dumbbell, and NGC 2346.

We also obtained an image of the Ring nebula with the new NOAO InSb array camera on the 2.1 m telescope at Kitt Peak, Arizona. This image, shown in Figure 5, was obtained through a standard K band filter. Our narrow-band UKIRT data on the Ring suggests that most of the K band flux seen in Figure 5 is due to a blend of many H_2 emission lines.

III. PHYSICAL CHARACTERISTICS OF PLANETARY NEBULAE

Analysis of the H_2 data presented in this paper touches upon virtually every aspect of PN with the exception of elemental abundances. Because of the vast and sometimes contradictory information contained in the literature on PN, we feel that it is appropriate to summarize, at the outset, that which is germane to the discussion in §§ IV and V. Pundits, perhaps, need not read this section!?

a) Density Structure

Some PN display a faint outer optical halo which surrounds the much higher surface brightness primary nebulosity. Observations and theory may both be used to constrain the relative volume densities in the primary and the halo of a given PN. For the simplest case of constant mass loss rate at constant velocity from the red giant progenitors of PN, the molecular hydrogen number density per cm^3, n_{H_2}, may be written conveniently as:

$$n_{H_2} = 6 \times 10^{16} \dot{M}/R^2 V_\infty \, , \qquad (1)$$

where $\dot{M}$ is the total mass-loss rate (including helium) in solar masses per year; R is the distance, in A.U., between the red giant and the cubic centimeter in question; and V_∞ is the terminal outflow velocity in km s^{-1}. Observations of red giants indicate that $\dot{M}$ is only very rarely, if ever, greater than 10^{-4} $M_\odot$ yr^{-1} (e.g., Morris 1985 and references therein). This is

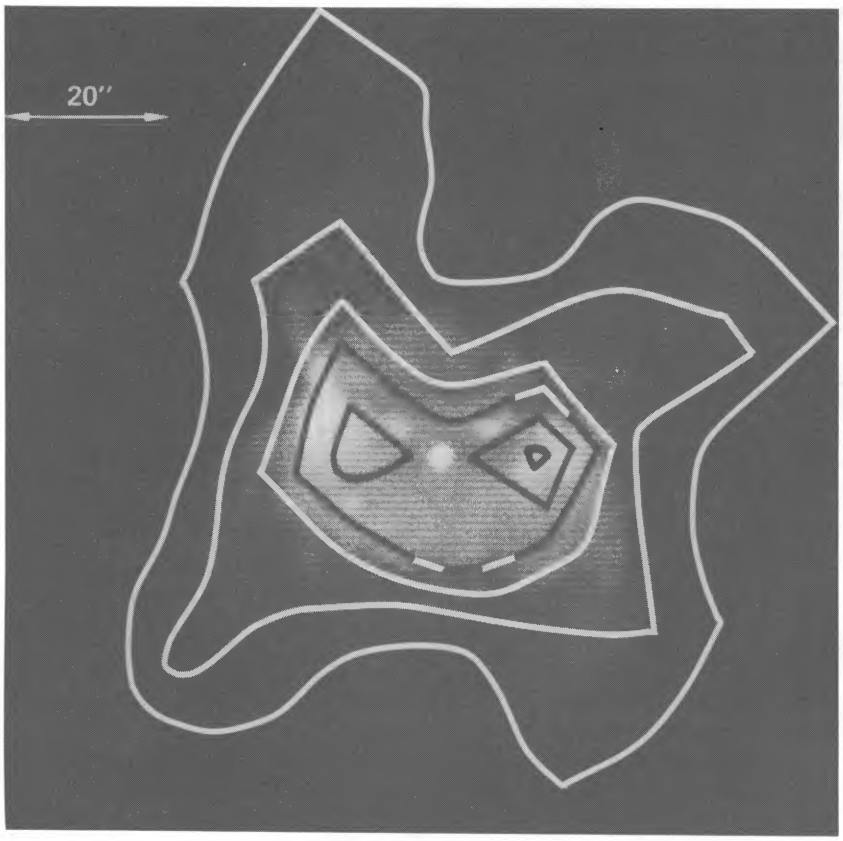

FIG. 3.—$S(1)$ $v = 1 \rightarrow 0$ contour map on an [N II] λ6584 photograph of NGC 2346 obtained by Dr. B. Balick with the KPNO 2.1 m telescope, the CCD camera and a 15 Å bandpass. See additional remarks in the legend to Fig. 2. The beam diameter for the $S(1)$ map was 12.″4, and the map points were separated by 6.″2. The contours are linearly spaced. The peak contour corresponds to 3.3×10^{-20} W cm^{-2} in a 12.″4 beam, and the spacing between contours is 0.55×10^{-20} W cm^{-2}. Apparent positional discrepancies between optical and $S(1)$ features that are $\lesssim 6''$ should not be trusted. North is toward the top, and east is toward the left.

consistent with the idea that radiation pressure on dust grains drives the mass loss, $\dot{M} \lesssim L_*/cV_\infty$, and that L_*, the luminosity of the underlying star, is never greater than 6×10^4 $L_\odot$, which is the maximum possible luminosity on the asymptotic giant branch (AGB). Indeed, this idea may be used to estimate upper limits to the distances to PN with measured molecular mass loss rates (Jura 1984*b*).

In shock models of excitation of H_2 discussed in § V*a*, the pre-shock H_2 density, n_0, is a very important parameter. A firm upper limit to n_0, at a given R, may be obtained from equation (1) by assuming $\dot{M} = 10^{-4}$ $M_\odot$ yr^{-1}. When observed H_2 emission originates outside the volume of the primary nebulosity, then, in the absence of extreme clumpiness, n_0 can be no greater than the volume density measured in the optical halo (if one exists) and may be less if the density of the optical halo has already been increased by the passage of a shock. Only a very few direct optical measurements of electron densities in PN halos exist. Jewitt, Danielson, and Kupferman (1986, hereafter JDK) measure mean electron densities (n_e) in five halos which correspond to $\dot{M} \approx 10^{-4}$ $M_\odot$ yr^{-1}. Since it is exceedingly unlikely that mass loss rates are this large in all PN, we suspect that the densities in these halos have been increased by passage of a shock. JDK measure n_e in the primary nebulae to be about 10 times larger than n_e in the halos and the size of the halos to be about twice the size of the primaries, so the run of density with R appears to roughly follow equation (1) in spite of the fact that, probably, both the primary and halo nebulosities have been compressed by the passage of a shock.

In our analysis in §§ IV and V*a*, we assume that $2n_0$ is equal to the electron density that has been measured optically, using [O II] and/or [S II], in the primary nebula. Based on the above discussion, we regard this as a conservative assumption in the sense that $2n_0$ might be much less than—but is unlikely to be greater than—n_e in the primary nebulosity unless, perhaps, the H_2 emitting volume is highly clumped (see, e.g., the model of Alcock and Ross 1986), and the H_2 emission originates in the clumps. Summarizing the justifications for setting $2n_0 = n_e$:

1. According to equation (1), n decreases as R^{-2} in an undisturbed flow.

2. Shocks, e.g., due to the collision of a fast and slow wind (see below), can increase the density in the primary nebula (but, by definition, will not increase the density, n_0, in the preshock gas).

3. Optical determinations of n_e from [S II] or [O II] tend to be biased toward regions of higher than average density (see, e.g., the discussion in JDK).

The degree of clumpiness of a typical PN is still a matter of debate. JDK, Schmidt and Cohen (1981), Capriotti, Cromwell, and Williams (1971), and Aller (1986) all argue that most PN are highly clumpy and/or filamentary, while Pottasch (1980) argues that clumping is, at most, modest.

b) Temperatures

In the primary nebulosity of a PN, electron temperatures are approximately 10^4 K. Some relatively cold regions containing

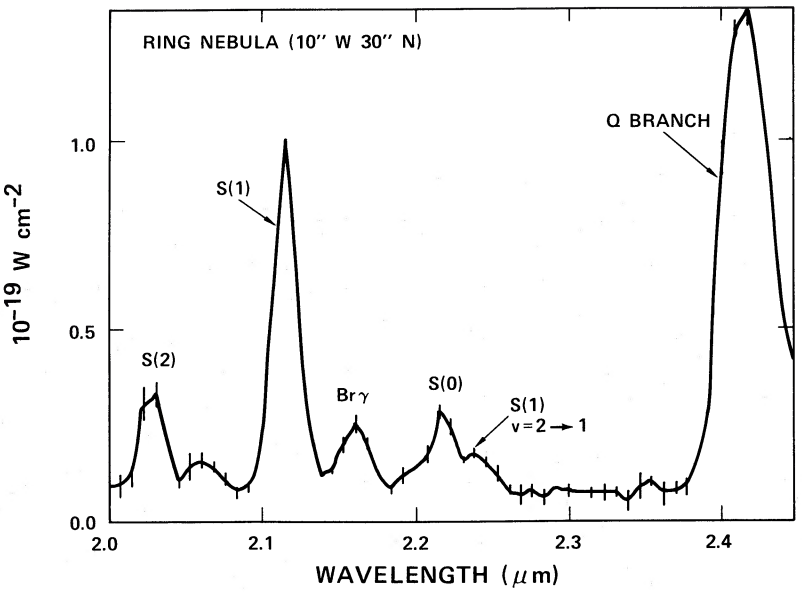

FIG. 4*a*

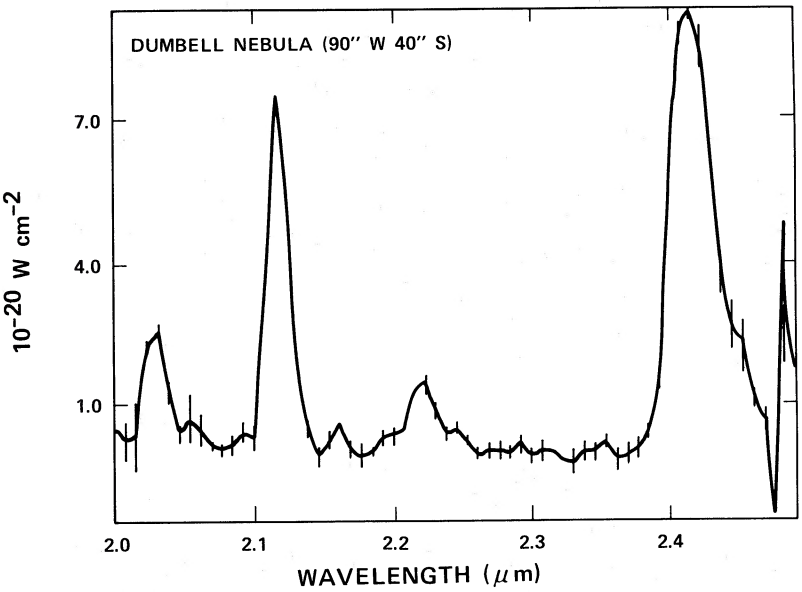

FIG. 4*b*

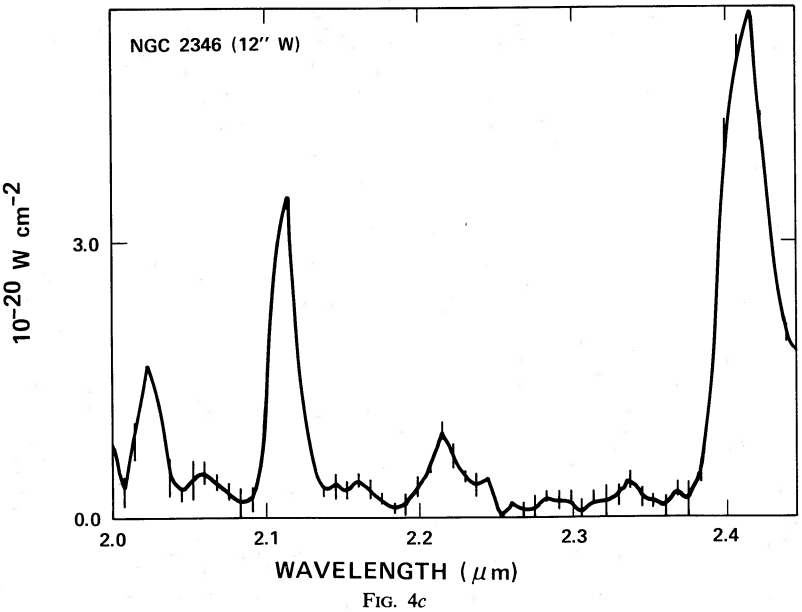

FIG. 4*c*

FIG. 4.—CVF spectra obtained at positions of peak $S(1)$ $v = 1 \rightarrow 0$ emission in the Ring, the Dumbbell, and NGC 2346. Offsets in arc seconds from the central star to the observed position are indicated in each panel. H Brγ and various spectral features from H_2 are indicated on the spectrum from the Ring. With the exception of the $v = 2 \rightarrow 1$ $S(1)$ line, all indicated H_2 lines are $v = 1 \rightarrow 0$ transitions. The spectra of NGC 2346 and the Ring have been normalized by dividing by a scan of BS 7615, and the Dumbbell spectrum was divided by BS 7796. Note that the units on the ordinate are power per spectral resolution element because the emission lines are not resolved by the CVF.

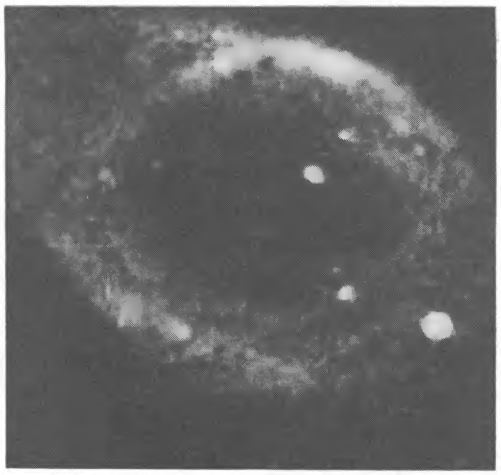

FIG. 5.—Image of the Ring nebula obtained through a standard *K* filter with an array camera on the 2.1 m telescope at Kitt Peak. The image is a mosaic of four frames, each of which contains 58 × 62 pixels. The scale at the telescope was 0".76 per pixel. The angular scale in the image agrees to within ~5% with the scale indicated on Fig. 2.

molecular gas may be embedded in the ionized primary near its periphery (Beckwith, Persson, and Gatley 1978).

Temperatures in halos, i.e., regions outside the primary optical nebulosity, are more uncertain. Occasionally, CO emission is observed which implies substantial quantities of cold molecular gas. More often, H_2 emission of the type described in this paper is detected, implying some gas at a few thousand degrees. Optical halos have been known for many years, but their high percentage of occurrence has been appreciated only relatively recently (e.g., JDK; Hippelein, Baessgen, and Grewing 1985; Balick 1986; Chu, Jacoby, and Arendt 1987). Proposals to explain the physical mechanism that excites this optical emission include the following:

1. The halos are reflection nebulosities. Light from the primary nebulosity and the central star is scattered off dust grains that are associated with the red giant winds discussed in § III*a* above.

2. The halos are photo-ionized and/or collisionally ionized and excited by Lyman-continuum photons and/or shock waves.

3. The halos are recombining ionized gas (Tylenda 1986). That is, as the ionizing luminosity of the central star declines (see § III*d* below), the outer portions of what was once the primary nebulosity become starved for ionizing photons and must cool and recombine.

Unfortunately, it is still not possible to decide, with certainty, among these three mechanisms. Indeed, different mechanisms may contribute in different PN. Critical measurements such as the relative optical spectra of primary and halo and the degree of polarization, if any, of the halo light have been carried out for only a few PN.

If the reflection nebulosity hypothesis is correct, then the halos are cool (i.e., not ionized). Depending on the size and density of a given halo, we estimate that the relative surface brightness, halo/primary, could conceivably range anywhere between 10^{-1} and 10^{-4}. Based on the absence of polarization at the wavelength of Hα, JDK concluded that the halos around the Ring nebula and one other PN are not reflection nebulosities. Based on the relative widths of [O III] and Hα lines in primary and halo nebulosities, Hippelein *et al.* concluded that the halos around three PN are not reflection nebulosities. Balick (1986) believes that the spectrum of halos is significantly more dominated by lines of low-excitation ions than are the primary nebulosities, again arguing against the reflection nebula hypothesis. On the other hand, Atherton *et al.* (1979) argue that the halo around NGC 7027 is a reflection nebulosity.

Since the optical halos in the Ring and the Dumbbell are located at or even beyond the region where we detect strong H_2 emission, photo-excitation and/or shock excitation of the optical lines is not easy to envision. If the halos are photoionized, for example, then either (1) the ultraviolet photons are leaking through holes in a clumpy or filamentary molecular cloud or (2) projection effects dominate the picture. Regarding possibility (1), the H_2 clumps would be embedded in a more tenuous gas with temperatures of approximately 10^4 K. Concerning possibility (2), we must remember that we are seeing a three-dimensional object of unknown shape projected onto the plane of the sky. Consider, for example, the bow tie–like PN sketched in Figure 6 (NGC 2346 seems to be an excellent approximation to this; see Figure 3 and discussion in § IV). If we rotate this sketch by 90° around an axis lying in the plane of the page and perpendicular to the line joining the two halves of the bow tie, then we would be looking approximately along the axis of a ring and the picture might well be dominated by something looking like the Ring nebula. The fainter bow tie nebulosities might then appear to spill out over the outer edge of the Ring thus producing a faint outer halo. However, Atherton *et al.* (1978) prefer to model the Ring Nebula as a spheroidal shell, and Goad (1975) thinks that it is most likely a cylinder with axis nearly parallel to the line of sight. It is not obvious that in either of these models simple projection effects alone (i.e., without, in addition, a clumpy, leaky ring of H_2) can produce the faint outer halo. In the Dumbbell nebula, it is not easy to visualize how projection effects alone can account for the roughly spherical halo.

Finally, consider the recombining halo model. It cannot easily explain the [O III] lines that are observed in halos around PN. In addition, the H_2 that we have detected in the Ring and the Dumbbell needs to have formed in the recombining phase since; in this hypothesis, all gas inside the halos previously was ionized when the central star was more luminous. At hydrogen densities of approximately 10^3 cm^{-3}, estimated rates for forming H_2 on either dust grains (Hollenbach, Werner, and Salpeter 1971) or via the H^- route (Black 1978) are orders of magnitude too slow compared with the dynamical expansion time (approximately a few thousand years) of the PN. Unless H_2 can be formed much more rapidly than is presently believed to be possible, the recombining halo model seems inapplicable to PN containing substantial amounts of H_2 and we consider it no more.

c) Magnetic Fields

To explain the H_2 emission from the Orion molecular cloud, various groups (e.g., Draine and Roberge 1982; Chernoff, Hollenbach, and McKee 1982) have appealed to C-type MHD shocks. These require large magnetic fields and very small ionization fractions. Neither condition is likely to be satisfied in the H_2 cloudlets that surround PN, although, in fact, direct observational support for this contention is very sparse. Reid *et al.* (1979) have estimated, from OH maser observations, magnetic fields in molecular envelopes around a few red giant stars. In U Ori, for example, they deduce a field of 10 mG at a distance of 10^{15} cm from the central star. Therefore, at a dis-

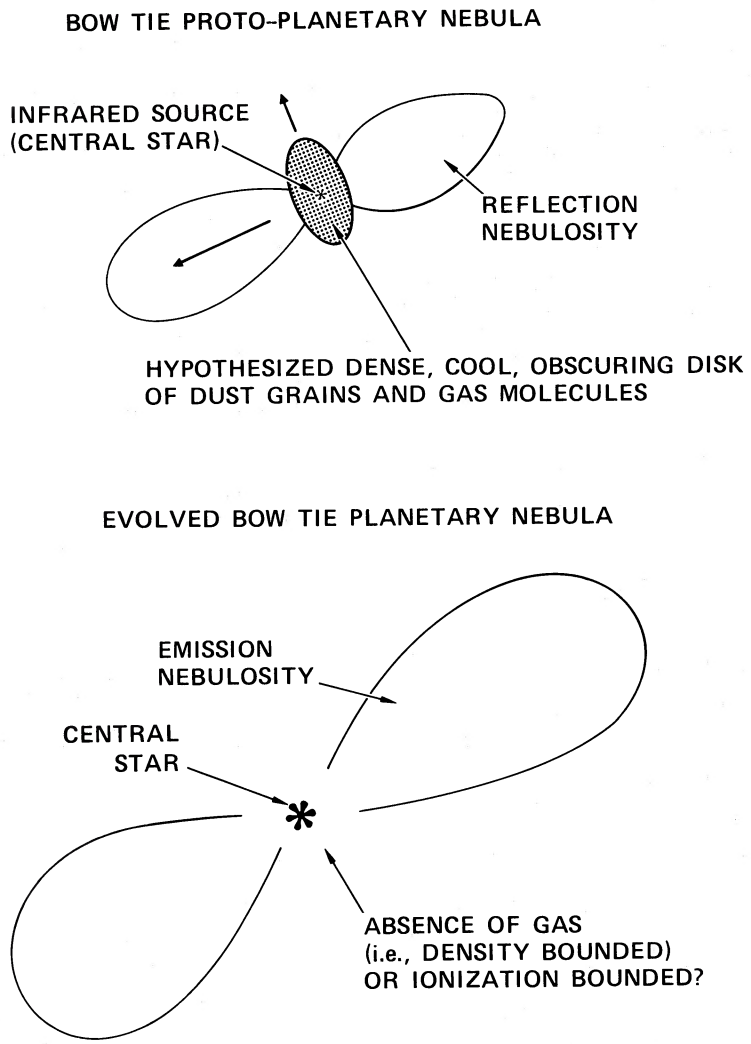

FIG. 6.—Sketch of young and evolved bow tie nebulae. Does the former, in fact, evolve into the latter? See § V*b* for discussion.

tance of, say, 10^{18} cm, the field would be $\lesssim 10^{-2}$ μG (the equality applies if the field is frozen into the mainly neutral outflowing gas). Since, according to equation (1), the H_2 density at this distance is approximately 10 cm^{-3} for a typical $\dot{M} \approx 10^{-5}$ $M_\odot$ yr^{-1}, the magnetic field is completely negligible. Therefore, we do not consider magnetic shocks in § V*a*.

d) Stellar Wind and Evolution of Central Star

Shock excitation of H_2 in NGC 7027 has been suggested to be due to the expansion of the ionized region (Beckwith *et al.* 1980) and, in AFGL 618, to fast winds driven by radiation pressure from the central star (Beckwith, Beck, and Gatley 1984; Persson *et al.* 1984). *IUE* measurements indicate that the central stars of various PN are driving fast winds (e.g., Cerruti-Sola and Perinotto 1985) with $\dot{M}$ much less than and V_∞ much greater than the values that obtain for these quantities when the star was on the AGB. The data are generally consistent with the relationship $\dot{M}V_\infty \approx L_*/c$, as expected for radiation pressure. The current stellar luminosities are often $\lesssim 10^3$ $L_\odot$ (e.g., Table 1 in this paper and Fig. 1 in Wood and Faulkner 1986), and we deduce (see § V*a*) that the force associated with these current winds is hopelessly insufficient to generate the shocked emission that we observe. Therefore, in the discussion in § V*a*, we assume that if a fast wind is providing the pressure that drives the shock that excites the H_2, then the wind carried a momentum equivalent to a luminosity equal to 3×10^4 $L_\odot$. This is the peak luminosity reached by a main-sequence star of approximately 4 $M_\odot$ when at the tip of the AGB (Fig. 7 in Iben and Renzini 1983), and it will be sustained for a few hundred years after the star leaves the AGB (Fig. 1*a* in Wood and Faulkner 1986). The justification for choosing this large mass (and luminosity) is given in § V*c* where we argue that most, perhaps all, PN that display H_2 emission originate from massive main-sequence stars, and such stars will evolve on a time scale that is short compared to the dynamical lifetime of the PN (e.g., Giuliani 1981; Wood and Faulkner 1986 and references therein).

IV. INDIVIDUAL NEBULAE

In this section we analyze our H_2 observations of the Ring, the Dumbbell, and NGC 2346 as well as Storey's (1984) observations of NGC 3132. We assume that the emission is excited by shocks for the following reasons. Our CVF spectra (Fig. 4) indicate that the ratio of the $S(1)$ transitions from the $v = 2 \rightarrow 1$ and $v = 1 \rightarrow 0$ manifolds is $\lesssim 0.1$, which is well below the value of 0.5 predicted by the UV radiative excitation model of Black

TABLE 1

OBSERVED AND DERIVED QUANTITIES

Planetary Nebula (1)	n_e (cm^{-3}) (2)	D (pc) (3)	$L[S(1)]^a$ ($L_\odot$) (4)	$S(1)^b$ Surface Brightness (5)	L_* ($L_\odot$) (6)	V_{HII} (km s^{-1}) (7)	V_{CO} (km s^{-1}) (8)	M_{HII} ($M_\odot$) (9)
NGC 2346	400	800	0.1	4.5×10^{-5}	25	40	$\lesssim 25$	0.05
NGC 3132	800	600	0.03	7×10^{-5}	80	14	?	0.027
NGC 6720 (Ring)	1000	600	0.07	7×10^{-5}	250	$\lesssim 30$	~ 24	0.05
NGC 6853 (Dumbbell)	300	270	0.2	3×10^{-5}	115	15, >30	?	0.13

[a] Integrated $S(1)$ luminosity.

[b] Average $S(1)$ surface brightness (ergs s^{-1} cm^{-2} sr^{-1}).

and Dalgarno (1976). The observed ratio of H Brγ to H_2 $S(1)$ ($v = 1 \rightarrow 0$) intensity that we measure in the Ring, the Dumbbell, and NGC 2346 (Fig. 4) is much less than the ratio given in Table 7 of Black, Porter, and Dalgarno (1981) in their associative detachment/UV model. Storey (1984) and Beckwith, Beck, and Gatley (1984) argue on similar grounds that H_2 emission from NGC 3132, AFGL 2688, and AFGL 618 is shock-excited. We assume that the 2 μm extinction is negligible toward all the PN that we analyze.

Properties of the four PN are summarized in Table 1. The second column lists representative electron densities for the primary optical nebulosities (§ III*a*). These n_e as well as the distances, D, to the PN have been gleaned from the literature. The distances are often poorly known but the major conclusions (or problems) of this paper are insensitive to the values assumed for D. The total $S(1)$ luminosities integrated over the maps are given in column (4). These may be slight underestimates of the true luminosities since we have not accounted for extended low surface brightness emission, should it exist. Conversion of these luminosities to total H_2 luminosities is uncertain and depends on preshock density (n_0) and shock velocity. Total H_2 luminosities are probably about one order of magnitude larger than those given in column (4).

The average $S(1)$ surface brightnesses given in column (5) apply over the areas shown in the H_2 maps. Estimates of current bolometric central star luminosities, corresponding to the distances given in column (3), are listed in column (6). Column (7) lists expansion velocities of the primary optical nebulosities taken from Table 1 in ZA. Column (8) gives expansion velocities for the remnant red giant wind as measured via CO microwave emission (Knapp 1985; Huggins and Healy 1986*b*; Huggins 1986). CO emission is not yet detected from the Dumbbell in spite of significant searches by Knapp (1986) and Huggins (1986). In column (9) we give estimates of the masses of the primary optical nebulosities that are consistent with the tabulated values of n_e and D.

a) The Ring Nebula (NGC 6720)

Figure 2 is a contour map of the $S(1)$ flux. We assume that the H_2 emission originates from a ring with inner and outer radii equal to 20″ and 40″, respectively. Then the total flux in the $S(1)$ line is approximately 7.2×10^{-19} W cm^{-2}. As mentioned above, the total H_2 emission integrated over all lines is probably approximately 10 times larger. The average surface brightness that corresponds to this total H_2 emission is approximately 60 times greater than the surface brightness in [N II] λ6584 that we estimate from data given by Goad (1975). Goad's measured surface brightness of [O I] λ6300 is 4 times smaller than that of [N II]. Corrections, due to extinction, of these measured [N II] and [O I] fluxes must be small since Hawley and Miller (1977) derive $A_V \lesssim 1$ mag at various positions in the Ring. Therefore, even if these atomic transitions are shock-excited, H_2 radiates away the bulk of the shock energy in the Ring. We assume that this is the case also in the other three PN in Table 1.

The total mass of hot H_2 in the $v = 1$ $J = 3$ level is approximately 10^{-6} $M_\odot$. An upper limit to the mass of *hot* H_2 (approximately 10^{-4} $M_\odot$) may be calculated by assuming a Boltzmann population distribution corresponding to 2000 K. Because of the low volume density, the hot H_2 will be subthermally excited and the total mass of hot gas will be less than this upper limit. The mass of H_2 responsible for the 2 μm emission lines is much smaller than either the mass of ionized gas (Table 1) or the mass of cold H_2 ($\gtrsim 0.005$ $M_\odot$) estimated by Huggins and Healy (1986*b*) to be associated with the CO that is observed from the Ring nebula. However, because the radiative lifetime of the vibrationally excited H_2 is roughly three orders of magnitude smaller than the dynamical lifetime of the PN and because shocked H_2 emission is detected from most PN at small galactic latitude (Table 4), the total mass of *cold* H_2 implied by our observations is comparable to the mass of cold H_2 given in the preceding sentence. The same argument applies to the H_2 observations of NGC 6853 and NGC 2346 discussed below.

Beckwith, Persson, and Gatley (1978) showed that, along one north-south line through the Ring nebula, the peak [O I] λ6300 and $S(1)$ emissions occur at the same radial offset from the central star and that this peak lies outside the peak Hβ and Bγ emission in the primary ring. In Table 2 we present additional data that confirm and extend their conclusion.

b) The Dumbbell Nebula (NGC 6853)

Figure 1 is a contour map of the $S(1)$ flux. We assume that the H_2 emission originates from a rectangle with dimensions of 4′ × 8′. The total flux in the $S(1)$ line is approximately 9×10^{-18} W cm^{-2}. Because the emission is so extensive compared with our 19″.6 beam, the map is somewhat undersampled, and small-scale details must be regarded with a bit of suspicion. For example, there clearly is a bright ridge of H_2 emission that runs through the central star from the northeast to the southwest coincident with the ridge of brightest surface brightness on optical photos (see, e.g., the 1983 July cover of *Sky and Telescope*). The H_2 emission peak located approximately 155″ north and approximately 75″ east of the central

TABLE 2

RING NEBULA DIMENSIONS[a] AND RELATIVE INTENSITIES[b]

	[O III] λ5007		H I λ4861		[N II] λ6584		[O I] λ6300		H_2 S(1)	
INVESTIGATOR	Major	Minor	Major	Minor	Major	Minor	Major	Minor	Major	Minor
Goad 1975	46″.5	42″.6	46″.5	45″.9	63″.9	51″.0	64″.6	54″.3	...	...
Atherton *et al.* 1978	46	49	53	52	63	59	70	64	...	...
Balick 1986	...	50	...	50.4[c]	...	54	74	64	...	...
This paper	...	...	...	...	...	...	...	...	75.4	66
Relative flux[b]	...	3.7	...	3	...	33	...	79	...	≳12

[a] Separation in arcsec between the peaks in surface brightness as measured along the major and along the minor axes.
[b] Relative flux between minor axis peaks of ring and center of nebula (from Atherton *et al.* 1978, except for H_2).
[c] Based on Hα rather than Hβ.

star is real. However, the apparent peak in Figure 1 at the position of the central star may be an artifact of our course sampling interval.

As in the case of the Ring nebula, the mass of hot H_2 is but a tiny fraction of the ionized mass of the primary optical nebulosity. The Ring is surrounded by a faint optical halo that has been known for many years (Duncan 1937). The Dumbbell is also surrounded by a giant faint halo which is much less well known and photographed.

c) *NGC 2346*

Figure 3 is a contour map of the *S*(1) flux. We assume that H_2 emission originates from a square with side 70″. The total *S*(1) flux is approximately 4×10^{-19} W cm^{-2}. The mass of hot H_2 is much less than the mass of ionized gas (Table 1) as well as the mass of cold H_2 ($\gtrsim 0.005\ M_\odot$) estimated by Huggins and Healey (1986*b*) to be associated with the CO that is observed from NGC 2346.

As in the Ring and the Dumbbell, the large-scale H_2 distribution in NGC 2346 is mostly external to but otherwise follows the primary optical contours remarkably well. In addition, there is clear evidence, in the form of maxima on either side of the central star, for the existence of a dense torus of H_2 lying in an approximately east-west plane and encircling the central star. We discuss this feature in § V*b*. A detailed model for the inner regions of NGC 2346 is described by Schaefer (1985).

We also measured broad-band photometric fluxes on the central star of NGC 2346 with two different beam sizes (see Table 3B) and mapped a region of 2′ (R.A.) by 2′ (decl.) with a 12″.4 beam at *K*. Our measured fluxes at the central star are remarkably flat in agreement with earlier measurements by Cohen and Barlow (1975). The most important aspect of our measurements for the purposes of the present paper is that the broad-band emission has a very different spatial distribution than the *S*(1) emission. In particular, the continuum emission is essentially a point source in a 7″.8 beam with perhaps some slight extension in the east-west direction.

d) *NGC 3132*

We utilize data from Storey (1984) and elsewhere to calculate the quantities listed in Table 1.

V. DISCUSSION

a) *Shock Excitation of* H_2

At the beginning of the previous section we argued that the observed *S*(1) line is shock-excited. Although, qualitatively, there can be little doubt that the excitation is via shocks rather than ultraviolet pumped fluorescence, a quantitative understanding of the shocks is not now possible for reasons that we summarize below.

We first assumed that excitation of the $v = 1$ level is via H_2–H_2 collisions and considered shocks of velocity V_s driven into molecular clouds of H_2 number density n_0 by the pressure of the expansion of ionized gas and also by fast stellar winds in both uniform and clumpy models. The H_2–H_2 excitation rates appear to be uncertain by an order of magnitude (there may even be an associated activation energy). For rates given in Table 1 in Lepp and Shull (1983) or Table 1 in Shull and Beckwith (1982), in no case were we able to find a plausible force that could produce sufficient pressure to drive a shock that could match the observed intensity of *S*(1) emission. We considered only the case of a momentum-conserving wind. In particular, the pressure required to drive the shock ($P_{\rm shock} =$

TABLE 3A

H_2 [*S*(1)] FLUXES (AND UPPER LIMITS)

Planetary Nebula	Position (Offsets from Center)		*S*(1) Flux (W cm^{-2}) into a 19″.6 Diameter Beam
NGC 650	15″W	15″S	0.5×10^{-20} (6 σ)
	20″W	0″S	0.3×10^{-20} (4 σ)
	0″W	20″S	0.2×10^{-20} (3 σ)
	0″	0″	$<0.2 \times 10^{-20}$ (3 σ)
	15″W	15″N	$<0.2 \times 10^{-20}$ (3 σ)
	0″E	20″N	$<0.2 \times 10^{-20}$ (3 σ)
	15″E	15″N	$<0.2 \times 10^{-20}$ (3 σ)
	20″E	0″N	$<0.2 \times 10^{-20}$ (3 σ)
	15″E	15″S	$<0.2 \times 10^{-20}$ (3 σ)
NGC 3587 (Owl)	0″	0″	$<0.3 \times 10^{-20}$ (3 σ)
	15″E	15″N	$<0.3 \times 10^{-20}$ (3 σ)
	30″E	30″N	$<0.3 \times 10^{-20}$ (3 σ)
	15″E	15″S	$<0.3 \times 10^{-20}$ (3 σ)
	30″E	30″S	$<0.3 \times 10^{-20}$ (3 σ)
	120″E	120″N	$<0.3 \times 10^{-20}$ (3 σ)
	120″E	120″S	$<0.3 \times 10^{-20}$ (3 σ)
NGC 4361	0″	0″	$<0.3 \times 10^{-20}$ (3 σ)
NGC 6058	0″	0″	$<0.3 \times 10^{-20}$ (3 σ)
NGC 6818	0″	0″	$<0.4 \times 10^{-20}$ (3 σ)

TABLE 3B

NGC 2346: PHOTOMETRIC MAGNITUDES

Color	7″.8 Beam	19″.6 Beam
J	10.59	10.50 (±0.03) (3 σ)
H	9.95	9.82 (±0.03)
K	8.87	8.82 (±0.03)
L	7.11	(±0.05)

$m_{H_2} n_0 V_s^2$) was between one and two orders of magnitude greater than the pressure produced by either a fast wind or expanding ionized gas in all our momentum-conserving models.[1]

Uncertainties in collision rates notwithstanding, useful constraints could be placed on the models if we knew V_s. However, according to Geballe (1986), the ratio of intensities in the $v = 2 \rightarrow 1$ and $v = 1 \rightarrow 0$ $S(1)$ transitions is found, empirically, to be independent of shock velocity over the range of interest to us here (i.e., $10 \lesssim V_s \lesssim 35$ km s^{-1}). Therefore, we cannot use line intensity ratios, such as those in Figure 4, to constrain V_s and a direct very high spectral resolution measurement of the width of the $v = 1 \rightarrow 0$ $S(1)$ line profile would be of great value.

Even more uncertain than the H_2–H_2 rates are those due to excitation of the vibrational levels by collisions between H and H_2. Measurements by Heidner and Kasper (1972) yielded rates at 300 K that are 4 times smaller than those estimated theoretically by Chu (see Table 1 in Shull and Beckwith 1982 or Lepp and Shull 1983). Dalgarno (1987) estimates that at 2000 K Chu's calculated rates might be as much as 40 times larger than the actual excitation rates. Since, at 2000 K, Chu's rates are approximately 3000 times larger than the H_2–H_2 rates given by Shull and Beckwith, H–H_2 collisions should dominate the excitation of the vibrational levels provided that of order a few percent of the hydrogen is atomic in the $S(1)$ radiating layers. The enormous uncertainties in the various rate coefficients preclude a more precise statement at this time. Nonetheless, we suspect that the observed brightnesses of the $S(1)$ lines can be understood only if the H_2 excitation is by collisions with H and n_H is at least a few percent of n_{H_2}.

Photodissociation of H_2 by radiation longward of the Lyman limit might produce this much H (e.g., Zuckerman, Terzian, and Silverglate 1980), but a detailed calculation is clearly called for. Since CO is more easily photodissociated than H_2, the relative paucity of CO in comparison with H_2 toward PN would be explained naturally. An alternative, albeit rather unlikely, mechanism for production of significant quantities of H in the $S(1)$ radiating regions is collisional dissociation of some H_2 in the shock. But this could occur for only a narrow range of shock velocities just below that required for complete dissociation of H_2. Since these shocks will not destroy CO directly (Roberge and Dalgarno 1982; Hollenbach and McKee 1980), its paucity in this picture needs to be accounted for. One possibility might be the endothermic chemical reaction $H + CO \rightarrow C + OH$. In any event, once formed, H will not recombine into H_2 during the dynamical lifetime of the PN (see remarks at the end of § III*b*).

If it were possible to measure both V_s and n_H in the $S(1)$ radiating region, then the H–H_2 collision rates could be derived. Observation of $S(1)$ emission with very high spectral resolution should yield V_s, but, unfortunately, detection of atomic hydrogen via its 21 cm transition will be, in general, exceedingly difficult if $n_H/n_{H_2} \lesssim 0.1$ (e.g., Zuckerman, Terzian, and Silverglate 1980). Recent measurements of 21 cm absorption toward a few PN (see Taylor and Pottasch 1987 and references therein) are suggestive, and perhaps the observational prospects are not entirely bleak.

[1] Higher pressures could, in principle, be produced with an energy-conserving wind (e.g., Kwok 1983; Kahn 1983). However, there is no observational evidence for soft X-rays from PN (see, e.g., the discussion following Kahn's paper) and hot bubbles may cool very rapidly in the PN environment (Harrington 1983; Harrington and Feibelman 1984).

b) Morphologies of Planetary Nebulae

The bipolar morphology characterizes approximately 50% of all PN (ZA[2]), as well as many "protoplanetaries" (e.g., AFGL 2688 and OH 231.8+4.2), a class of objects in which the central star is still insufficiently hot to ionize the surrounding circumstellar envelope. To arrive at this percentage, ZA included all PN that have a "bow tie" appearance (see Fig. 6 in the present paper), as well as ringlike PN (such as NGC 6720), that display two brightenings along a given axis (usually the minor one). In the following discussion we ignore the bipolar nature of many ringlike PN and consider all rings as one morphological class and all bow tie PN as another class.

For the bow tie class of protoplanetaries, the most popular model includes a dense torus (bagel) composed of gas and dust grains that surrounds the central star. The bow tie reflection nebulosities are produced by light escaping from the poles of the torus that illuminates lower density material previously ejected by the central star (Fig. 6). The star itself is seen only in the infrared because it is shielded by dust grains in the dense torus.

Although some PN superficially resemble bow tie protoplanetaries, it is not at all obvious that they should! This is because for a large *evolved* PN such as the Dumbbell, we would expect, based on the above model, to see something that looks more like the Ring nebula; the lower density, higher velocity bow tie–like blobs should have expanded away into space leaving behind the dense torus to be illuminated by the central star of the PN. (In an axially symmetric nebula, the polar expansion velocity is typically 1.5–2 times larger than the equatorial velocity [Wilson 1958; Khromov and Kohoutek 1968].)

The observations reported in this paper were motivated in part as a test of this morphological model. We wanted to determine if there is still unobserved neutral gas surrounding the narrow neck of evolved bow tie PN or if we really are seeing all the recently ejected gas in the currently photoionized regions (i.e., is the PN density bounded in all directions?).

We mapped two bow tie PN in detail, the Dumbbell and NGC 2346. NGC 2346 appears to be ionization-bounded over its entire surface and the hypothesized dense molecular torus is clearly shown in the $S(1)$ map (Fig. 3). No such structure is immediately evident in the $S(1)$ map of the Dumbbell (Fig. 1), but this is because the underlying optical photograph does not show the two faint lobes that appear in deep exposures and that lie along a line that runs SE to NW. That is, the bright optical nebulosity visible in Figure 1 is actually the dense torus, which is remarkable considering its enormous angular extent. In any event, after this paper was completed, we learned that Balick (1987) has developed a sophisticated evolutionary scheme to explain PN morphologies that is based on his high-quality, multi-ion CCD images and we defer to his paper for additional details.

Generally, bow tie nebulae do display relatively intense H_2 emission. In Table 4, eight bow tie nebulae have detectable H_2 emission (albeit weakly in NGC 650), whereas at most one, the Owl nebula (NGC 3587), does not. (We say "at most one"

[2] Two printer errors in the Appendix of ZA were not corrected in proof. In the expression for μ, the quantity $(\Delta E/KT_0)$ in the first term on the right-hand side should be squared. Also, three lines above eq. (A3), the "effective recombination coefficient" is $N_e N_i \alpha_{nn'}$, not simply $\alpha_{nn'}$ as printed. In addition to these errors, Soker *et al.* 1984, *M.N.R.A.S.*, **210**, 189 was omitted from the list of references.

TABLE 4

H_2 EMISSION IN PLANETARY NEBULAE

Object (1)	PK (2)	Type[a] (3)	Beam Size (4)	$S(1)$[b] Surface Brightness (5)	Wind? (6)	Optical Halo? (7)	V_{LSR} (km s^{-1}) (8)
A. Planetary Nebulae with H_2 Emission							
NGC 650	130 − 10°1	BT	19″.6 diameter circle	7×10^{-6}	...	...	−16
AFGL 618	...	BT	8″ diameter circle	14×10^{-4}	...	...	−23
J900	194 + 2°1	BT + D	12″ diameter circle	8×10^{-5}	...	...	34
NGC 2346	215 + 3°1	BT	12″.4 diameter circle	1.2×10^{-4}	...	...	5
NGC 2440	234 + 2°1	BT	12″ diameter circle	9×10^{-5}	...	...	45
NGC 2818	261 + 8°1	BTI	14″ × 5″ rectangle	7×10^{-5}	...	...	−17
NGC 3132	272 + 12°1	R	14″ × 5″ rectangle	2.2×10^{-4}	Maybe	Yes	−28
IC 4406	319 + 15°1	D	14″ × 5″ rectangle	$\sim 10^{-4}$	...	...	−40
NGC 6072	342 + 10°1	...	14″ × 5″ rectangle	$\sim 10^{-4}$	...	...	13
NGC 6720	63 + 13°1	R	19″.6 diameter circle	1.2×10^{-4}	No	Yes	0
BD 30°3639	64 + 5°1	D	10″ diameter circle	1.8×10^{-4}	...	Yes	−13
NGC 6853	60 − 3°1	BT	19″.6 diameter circle	1.0×10^{-4}	No	Yes	−24
AFGL 2688	...	BT	5″ diameter circle	3.8×10^{-4}	...	...	−35
NGC 7027	84 − 3°1	R	10″ diameter circle	7.4×10^{-4}	...	Yes	24
NGC 7293	36 − 57°1	CR	14″ × 5″ rectangle	4×10^{-5}	No	Yes	−25
HB 12	111 − 2°1	AMI	10″ diameter circle	1.6×10^{-4}	...	...	5
B. Planetary Nebulae without Detected H_2 Emission							
NGC 246	118 − 74°1	R + D	14″ × 5″ rectangle	$<5 \times 10^{-6}$	No?	...	−51
NGC 1360	220 − 53°1	AM	14″ × 5″ rectangle	$<7 \times 10^{-6}$	No	...	26
NGC 1535	206 − 40°1	R	14″ × 5″ rectangle	$<10^{-5}$	...	Yes	−20
IC 418	215 − 24°1	R	14″ × 5″ rectangle	$<10^{-4}$	Yes	...	43
NGC 2792	265 + 4°1	...	14″ × 5″ rectangle	$<1.3 \times 10^{-5}$	...	...	−1
NGC 3195	296 − 20°1	...	14″ × 5″ rectangle	$<1.3 \times 10^{-5}$	...	...	−20
NGC 3242	261 + 32°1	R	14″ × 5″ rectangle	$<2 \times 10^{-5}$	...	Yes	−5
NGC 3587	148 + 57°1	D + BT?	19″.6 diameter circle	$<4 \times 10^{-6}$	...	...	12
NGC 4361	294 + 43°1	AM	19″.6 diameter circle	$<4 \times 10^{-6}$	No	Yes	8
Me 2-1	342 + 27°1	...	14″ × 5″ rectangle	$<10^{-5}$	...	...	45
NGC 6058	64 + 48°1	R	19″.6 diameter circle	$<4 \times 10^{-6}$	...	Yes	20
NGC 6153	341 + 5°1	...	14″ × 5″ rectangle	$<2 \times 10^{-5}$	...	...	45
NGC 6572	34 + 11°1	R + AM	10″ diameter circle	$<1.4 \times 10^{-4}$	Yes	...	10
NGC 6790	37 − 6°1	*	10″ diameter circle	$<10^{-4}$	...	...	57
NGC 6818	25 − 17°1	R	19″.6 diameter circle	$<5 \times 10^{-6}$	...	...	−1
IC 4997	58 − 10°1	*	10″ diameter circle	$<1.4 \times 10^{-4}$	...	...	−50

[a] Morphological type designations are similar to those in Table 1 of ZA except that BT(here) = BP(ZA); BT: bow tie; R: ring; CR: complex ring; D: disk; AM: amorphous; I: irreguar; *: stellar. The H_2 data are from the present paper; Storey 1984; Beckwith, Persson, and Gatley 1978; Beckwith, Beck, and Gatley 1984; Beckwith *et al.* 1980; and Isaacman 1984.

[b] Peak $S(1)$; $v = 1 \rightarrow 0$; surface brightness (ergs s^{-1} cm^{-2} sr^{-1}).

because the morphology of the Owl is unusual, and it may not be a true bow tie in spite of its classification as such by ZA.) We therefore conclude that bow tie PN are generally ionization-bounded in agreement with expectations of the morphological model described above. Observations (maps) of most of these PN are as yet insufficient to delineate the existence of a dense molecular ring at the neck of the bow tie.

Livio, Salzman, and Shaviv (1979) and Morris (1981) argued that bipolar and elliptical symmetries in PN are due to the gravitational field of a close binary companion to the red giant progenitor of the PN. ZA argued against this idea but were unable to arrive at a definitive conclusion. In particular, they did not find any strong dependence between a given morphological shape and the mean absolute galactic latitude of those PN that display the given shape (see their Table 3). With the clue supplied by our Table 4 that bow tie nebulae (excepting the Owl) appear to have small galactic latitudes, we have gone back and reanalyzed data in Table 1 in ZA. We find that bow tie PN do indeed have significantly smaller galactic latitudes than does the average PN (compare the mean galactic latitude for bow tie PN given in our Table 5 with the mean galactic latitudes of all PN [ZA Table 3]). Therefore, we conclude that bow tie nebulae are associated with progenitor stars that were massive when they were on the main sequence. In addition, as we argue from both theory and observation in § V*c* below, the intrinsic luminosity of a PN that is excited by a central star that was once a massive main-sequence star is likely to be *less*

TABLE 5

H_2 EMISSION, BOW TIE MORPHOLOGY, AND GALACTIC LATITUDE

PN Class	Galactic Latitude (mean absolute value)	Standard Deviation[a]	n[b]
With H_2 emission	6°.8	4°.4	15[c]
Without H_2 emission	29.4	21.2	16
Bow tie morphology	5.1	5.2	22[d]

[a] The standard *error* of the mean is $(n)^{1/2}$ times smaller than these standard deviations. Therefore, it is clear that PN without H_2 emission constitute a population different from bow tie PN and PN with H_2 emission.

[b] Number of PN.

[c] Excluding NGC 7293 (see discussion in text, § V*c*).

[d] Excluding NGC 3587 (see discussion in text, § V*b*).

than the luminosity of a PN that originates from a lower-mass star. Therefore, for a given mean $|b|$, PN from massive stars actually lie *closer* to the galactic plane than do PN from low-mass stars.

Bow tie nebulae are precisely the type of objects considered by Morris (1981) who argued that the bow tie shape is due to the gravitational field of a close companion star. Since the above argument establishes, reasonably securely, that bow tie PN come from relatively massive progenitor stars, it follows that Morris's model can be correct only if close companions are significantly more likely to be found near massive stars than near lower mass stars. We can think of two effects that are consistent with this possibility; however, both seem to be too weak to explain the correlation with galactic latitude.

Abt and Levy (1976) suggest that Population II stars are deficient in close doubles (separation $\lesssim 0.5$ A.U.) when compared with Population I stars. If so, massive stars that become PN might have relatively more of the close companions required in Morris's model. Although exact quantitative data are lacking, we suspect that, over the range of main-sequence masses, 1–7 $M_\odot$, of relevance to formation of PN, this effect will be too weak to explain the $|b|$ dependence of morphological type in nearby disk PN. The second effect is related simply to the size of a star when on the AGB. The radius (R_*) of an AGB star that had a massive main-sequence progenitor is approximately 3 times larger than the radius of an AGB star with a low-mass progenitor. From Table 2 in ZA and the discussion in § II of ZA, we estimate that the probability of finding a close companion, in the sense that the star-star separation is $\lesssim 1.3\ R_*$, is $\lesssim 1.5$ times greater near a massive star as compared to a low-mass star. Again, this seems to be too weak an effect to account for the obvious dependence of bow tie morphology on galactic latitude.

Antithetical to these two effects is the fact that AGB stars at low galactic latitude have larger mean outflow velocities, V_∞, than do AGB stars at larger $|b|$ (Zuckerman, Dyck, and Claussen 1986; Zuckerman and Dyck 1987). The gravitational effect of a given close companion must be inversely correlated with V_∞ and, hence, with $|b|$. Therefore, although it is not yet possible to make a rigorous quantitative case, we believe that it is unlikely that bow tie morphology is, in general, a signpost for close companion stars. Rather, the bow tie form is associated with massive stars. This association was first noted by Calvert and Peimbert (1983) in connection with Peimbert's PN of type I (Peimbert and Torres-Peimbert 1983). These authors seemed unaware of the papers by Livio *et al.* and by Morris and, therefore, did not discuss the close companion star model at all. Rather, Calvert and Peimbert argued that rapid rotation in massive main-sequence progenitors (spectral type A5 and earlier or $M \gtrsim 2.4\ M_\odot$), is responsible for the bow tie morphology. We think that the arguments in favor of this model are exceptionally weak, as we now outline.

Calvert and Peimbert (1983) remark that rotational velocities of massive main-sequence stars are approximately 200 km s^{-1}. By the time these stars expand to become luminous AGB stars ($R_* \approx 5$ A.U.), their surface velocities are likely to be $\lesssim 1$ km s^{-1}, which is but a miniscule fraction of both the escape velocity from the surface (approximately 40 km s^{-1}) and of V_∞(~ 20 km s^{-1}). (Unfortunately, direct measurements of surface rotation rates of AGB stars do not yet exist, so we simply assume conservation of angular momentum in the expanding star.) Therefore, in the absence of some leverage effect that is a very strong function of surface velocity, one could safely conclude that rotation is *not* responsible for so pronounced a phenomenon as the bow tie morphology. In fact, some models for ejection of material from red giants to infinity, such as radiation pressure on dust grains (e.g., Jura 1984*a*; Zuckerman 1980 and references therein), *may* be sensitively dependent on surface velocity because of difficulty in levitating gas to a height at which dust grains can easily form. Because we do not yet understand the ejection process in detail, this question is still open.

A second weakness in the Calvert and Peimbert (1983) model is their apparent assumption that rapid rotation would produce a bow tie rather than some other common axially symmetric morphology (such as a ring, for example). In particular, the theoretical models of Phillips and Reay (1977), which Calvert and Peimbert appear to favor, produce a literal zoo of different morphologies. Why select only the bow ties from this zoo? Ring-like PN, for example, do not show any obvious preference to lie at small galactic latitude (see above discussion in conjunction with Table 3 in ZA), and yet rings would seem to follow quite naturally from the "focusing toroids" that are an essential part of the Calvert/Peimbert model.

In summary, existing models that explain bow tie morphology in terms of either the gravitational field of a close companion star or rapid stellar rotation at present have little or no observational and/or theoretical support. Among the "buzzwords" that have appeared in the literature, this leaves magnetic fields and/or nonradial pulsations as potential explanations of the bow tie phenomenon.

c) *Evolution of Planetary Nebulae and Their Central Stars*

In Table 4 we list the various PN that have been searched for H_2 emission for which we are able to estimate peak $S(1)$ surface brightnesses (or upper limits). The table is divided according to whether the $S(1)$ line has or has not been detected. In no sense should it be regarded as the last word on the presence or absence of H_2 emission since the limits are very nonuniform (e.g., compare Storey's 1984 nondetection of IC 418 with our detection of NGC 650). Nonetheless, correlations discussed in § V*b* and below are so striking that we doubt that future, more uniform, surveys will overturn our conclusions. In particular, as summarized in Table 5, the mean galactic latitude of PN with detected H_2 is substantially smaller than the mean $|b|$ for PN without H_2. We interpret Table 5 to indicate that ionization-bounded PN tend to originate from stars that were relatively massive when they were on the main sequence. We have not included the Helix in Table 5 because it is very close to the Sun and is located quite close to the galactic plane in spite of its large galactic latitude.

Analyses of CO emission from circumstellar envelopes around luminous, infrared-bright, AGB stars indicate that typically $\dot{M}V_\infty \approx L_*/c$ (e.g., Jura 1983; Morris 1985; Zuckerman and Dyck 1986). Once an AGB star has achieved such a large $\dot{M}$, the hot core must soon become exposed and a PN results. If L_* remains constant over the observable lifetime of the PN, then, except for a very narrow range of L_*, a circumstellar envelope with a density profile $\propto R^{-2}$ (eq. [1]) will either be fully ionized or not ionized, depending on the number of ionizing photons emitted by the central star (Wright and Barlow 1975). Therefore, if the ionizing luminosity of the central star remains constant, one would predict that very few large, ionization-bounded PN exist. Since $\dot{M}/L_*$ is roughly constant, i.e., independent of L_*, this prediction is largely independent of the initial core mass.

Calculations indicate, however, that the ionizing photon luminosity of massive central stars declines by as much as two orders of magnitude over the dynamical lifetime of the PN (e.g., Giuliani 1981; Wood and Faulkner 1986 and references therein). For lower mass stars, the ionizing luminosity declines only after the PN is very far from the star and no longer visible. This accounts in a natural way for the association of ionization-bounded PN with massive stars and density-bounded PN with lower mass stars. It also explains why we observe shock-excited, rather than ultraviolet-pumped fluorescent, H_2 emission. That is, since the central stars of PN are intense sources of ultraviolet photons, one might wonder why we see no evidence for UV excitation similar to that now being detected near various reflection nebulae and H II regions (Gatley *et al.* 1987; Gatley and Kaifu 1986). The explanation, no doubt, lies in the rapid temporal variation of the PN central star luminosities (no such variations occur in young O and B stars). That is, UV excitation is due to the *current*, small, central star luminosity (light travel time is less than one year from the central star to radiating H_2), whereas shock excitation involves the dynamical transport (characteristic time scale of thousands of years) of large mechanical pressures that were established when the central star was much more luminous.

The brief period of high luminosity and high effective temperature, $T_{\rm eff}$ (see Fig. 1*a* in Wood and Faulkner 1986), could have an additional important consequence for H_2 emission from PN that originate from massive main-sequence stars. In § V*a* we argued that the $v = 1$ level is probably excited mainly by collisions with H atoms. Inspection of the evolutionary tracks for massive central stars suggests that most of the photodestruction of H_2 that produced these H atoms could have occurred during the period of high L_* and high $T_{\rm eff}$ rather than later after L_* declines dramatically. Detailed evolutionary calculations are required to clarify this point.

Specific evolutionary tracks have been calculated by Wood and Faulkner (1986) for a variety of assumptions (their Fig. 1). In two sets of tracks, their Figures 1*c* and 1*d*, rapid mass loss, $\dot{M} \approx 3 \times 10^{-5}\ M_\odot\ {\rm yr}^{-1}$, was assumed to continue until $T_{\rm eff}$ was larger than 10^5 K. A variety of infrared continuum and millimeter wavelength CO rotational line data (e.g., Zuckerman and Dyck 1986; Jura 1986*a*; Likkel *et al.* 1987; Zuckerman and Lo 1987) implies that many, probably most, and possibly all, post–AGB stars terminate rapid mass loss while $T_{\rm eff}$ is still quite low ($\lesssim 10^4$ K). For example, regarding the IR continuum data, by comparing the 12, 25, 60, and 100 μm fluxes in the *IRAS* point source catalog for a given post–AGB star, one can trace the history of mass loss during approximately the past 1000 yr. That is, dust grains that radiate at 100 μm were ejected from the star about 1000 yr ago, whereas dust that radiates at 12 μm was ejected only very recently so that stars with *IRAS* fluxes that peak at 25 or 60 μm are undergoing rapid declines in $\dot{M}$. When known, the spectral type of the underlying star usually lies somewhere in the range K through F.

What is the cause of the dramatic decline in $\dot{M}$? One conceivable possibility is cessation of pulsations of the underlying star since pulsations are probably essential for rapid mass loss from AGB stars (e.g., Jura 1986*b* and references therein). Indeed, van der Veen *et al.* (1987) have argued that OH/IR stars that have stopped pulsating have rapidly declining mass-loss rates and are just beginning to evolve off the AGB. We have checked the variability status (when known) of the stars that are listed in the references in the preceding paragraph. Except for the RV Tauri stars, discussed by Jura (1986*a*), pulsations have apparently stopped or diminished in most cases. In the case of the low-metallicity RV Tauri stars, declining mass-loss rates perhaps can be attributed to dust-to-gas ratios that are so small that the outward acceleration due to radiation pressure on dust grains does not exceed the gravitational force (Jura 1986*a*, *b*). In particular, as an RV Tauri evolves to larger $T_{\rm eff}$, it may become progressively more difficult for grains to form in the circumstellar material.

Wood and Faulkner (1986) note that the "observed" luminosities of PN nuclei with $T_{\rm eff} \approx 3 \times 10^4$ K disagree badly with the evolutionary tracks in their Figure 1 and indeed all theoretical tracks beginning with those of Paczyński (vintage 1970). They, therefore, argue that the "observed" luminosities are systematically in error by at least a factor of 3 which could, presumably, be attributed to an incorrect distance scale to the PN. The evidence for rapidly declining $\dot{M}$ at low $T_{\rm eff}$ discussed above then raises a disquieting possibility. Suppose that declining $\dot{M}$ were due to a corresponding decline in L_* rather than to cessation of stellar pulsations or insufficient dust in the circumstellar envelope. Then the implied post–AGB luminosities at $T_{\rm eff} \approx 10^4$ K would match well the "observed" luminosities of the nuclei of PN with $T_{\rm eff} \approx 3 \times 10^4$ K as plotted in Figure 1 of Wood and Faulkner (1986). When the distances to PN and the luminosities of post–AGB stars with declining $\dot{M}$ are established reliably, then this potential conflict between theory and observation can be resolved.

d) Ionization or Density-bounded?

The question of whether a given PN is ionization-bounded or density-bounded can enter into calculations of quantities such as the distance to a PN or He and H Zanstra temperatures. Researchers have employed various clever techniques to deduce whether a given PN is ionization-bounded or density-bounded (see, e.g., § IV in Pottasch 1980 for a summary). A complete map of H_2 emission over the surface of a PN, such as those in Table 1, can show unambiguously that the PN must be ionization-bounded in most but (since we do not know the three-dimensional structure) not necessarily all directions. Absence of $S(1)$ emission is somewhat more ambiguous since it could, for example, be due to the absence of a force to drive a shock rather than the absence of H_2.

In Table 6 we compare the H_2 results given in Table 4 with some previous tabulations that concern themselves with whether a given PN is ionization-bounded or density-bounded. Kaler (1983) compares H and He Zanstra temperatures, while Pottasch (1980) and Daub (1982) use arguments that depend on the masses of PN. We have also examined the relative fluxes listed by Kaler (1976, 1986), Aller and Czyzak (1979), and Torres-Peimbert and Peimbert (1977). By comparing the strengths of low-excitation ions such as [O I] λ6300 and [N II] λ6584 with Hα and Hβ, we have, essentially, guessed whether the PN are ionization-bounded or density-bounded. Although the H_2 data are still sparse and nonuniform, it appears that agreement with the Zanstra temperature technique is very good. The Owl (NGC 3587) is the only PN out of 10 for which the H_2 and Zanstra techniques disagree. Agreement between the presence of H_2 and the strength of the low-excitation forbidden lines is also generally good. However, there is little or no agreement between the H_2 observations and techniques that rely on nebula mass. This is very probably because Drs. Daub and Pottasch have not con-

TABLE 6

IONIZATION-BOUNDED AND DENSITY-BOUNDED PLANETARY NEBULAE

Object (1)	H_2 (2)	Ionized Mass P1980[a] (3)	Ionized Mass D1982[b] (4)	[O I], [N II], etc. (5)	H and He Zanstra Temperature (6)
NGC 246	d	d[c]	d	d	d
NGC 650	i(?)	...	d	i	i(?)
NGC 1360	d	...	d	d	d
NGC 1535	d	i	i(?)	d	...
IC 418	d(?)	...	i	i(?)	...
J900	i	...	i	d(?)	...
NGC 2346	i	i	d	i	...
NGC 2440	i	...	d(?)	i	...
NGC 2792	d	...	i	d	...
NGC 2818	i	...	d	i	...
NGC 3132	i	i	d	i	...
NGC 3195	d	...	d	?	...
NGC 3242	d	i	i	d	...
NGC 3587	d	i[c]	d	i(?)	i
NGC 4361	d	...	d	d	d
IC 4406	i	...	d	i	i
Me 2-1	d	...	i	d	...
NGC 6058	d	...	d	d	d
NGC 6072	i	...	d	...	...
NGC 6153	d	...	i	d(?)	...
NGC 6572	d(?)	i	i	d(?)	...
NGC 6720	i	i	d	i	i
NGC 6790	d(?)	...	i	d	...
BD 30°3639	i	i	i	i	...
NGC 6818	d	...	i	d(?)	...
NGC 6853	i	i[c]	d	i	i
IC 4997	d(?)	...	i	d(?)	...
NGC 7027	i	...	i	i	...
NGC 7293	i	i[c]	d	i	i

[a] Pottasch 1980.
[b] Daub 1982.
[c] From Zanstra temperature not from ionized mass.

sidered the strong variation of ionizing luminosity from massive central stars as PN evolve.

VI. CONCLUSIONS

Molecular hydrogen emission is detectable from a substantial fraction of PN and is, therefore, a useful probe to distinguish between ionization-bounded and density-bounded nebulae. Complete maps are especially valuable in elucidating the morphology of the PN. In the future, such maps could be mass-produced using array cameras on large telescopes. A valuable theoretical exercise that should accompany such maps is a time-dependent calculation of the H_2 and CO abundances in the molecular envelope. The primary conclusions of the current investigation are as follows:

1. $S(1)$ emission from H_2 closely follows the optical morphology of the Ring, the Dumbbell, and NGC 2346. The H_2 emission is more extended than the main emitting mass of ionized gas and, in NGC 2346, there is evidence for a dense torus of hot H_2 surrounding the central star.

2. The H_2 emission appears to be shock-excited. We considered shocks driven into molecular clouds by the pressure of the expansion of ionized gas and also by fast stellar winds in both uniform and clumpy models. When we assumed that the $v = 1$ level of H_2 is excited by collisions with other H_2 molecules, in no case were we able to find a plausible force that could drive a shock that could match the observed intensity of $S(1)$ emission. Vibrational excitation rates due to collisions of H with H_2 are very uncertain, but this type of collision could explain our observations if a modest percentage of the hydrogen is in atomic form in the shocked layers.

3. PN with observable H_2 emission (i.e., ionization-bounded) are preferentially found at smaller galactic latitude than are those that lack H_2 emission (i.e., density-bounded). This observation is consistent with theoretical stellar models that indicate a rapid decline in the flux of ionizing photons from the central stars of PN that originate from massive main-sequence stars. This rapid decline also explains, in a natural way, why we observe shock-excited, rather than ultraviolet-pumped fluorescent, H_2 emission.

4. PN with "bow tie" symmetry generally display H_2 emission, consistent with expectations of the most popular morphological model for these nebulae.

5. Bow tie nebulae are, on average, located at smaller galactic latitude than the general population of PN. When combined with the lower intrinsic luminosity of the central stars of PN from massive stars (conclusion [3], above), this implies that bow tie PN originate from stars that were massive when they were on the main sequence. Unless massive stars are accompanied by an inordinate number of close companion stars relative to low-mass stars, which seems unlikely, then bow tie morphology is a function of stellar mass and is not due to the gravitational field of a close companion star as postulated in some previous morphological models. Because of the relatively rapid rotation of massive main-sequence stars relative to low-mass stars, it has been suggested that this rapid rotation is, in part, responsible for the bow tie morphology. The evidence in support of this model is very weak or even nonexistent. Alternative possibilities include stellar magnetic fields and nonradial pulsations. But basically, we do not understand the physical mechanisms that shape PN.

6. Radio molecular and infrared continuum data imply that many, probably most, and possibly all, post–asymptotic giant branch (AGB) stars terminate rapid mass loss while the star still has a fairly low effective temperature ($T_{\rm eff}$). Therefore, evolutionary tracks for post–AGB stars that assume continued rapid mass loss when $T_{\rm eff} \gtrsim 10^4$ K are unlikely to be correct. If the standard evolutionary tracks for post–AGB stars that run at constant luminosity to large $T_{\rm eff}$ ($\gtrsim 10^5$ K) are correct, then the termination of rapid mass loss must be due to cessation of stellar pulsations and/or small dust-to-gas ratios in the circumstellar material.

7. There is a variety of techniques for distinguishing between ionization-bounded and density-bounded PN. The presence or absence of H_2 emission correlates well with techniques that rely on (1) comparative H and He Zanstra temperatures, or (2) strong forbidden line emission from low-excitation species such as [O I] λ6300 or [N II] λ6584. Techniques that rely on estimates of nebular masses are generally not in agreement with the H_2 observations probably because these estimates have neglected the effect of the rapid decline in central star luminosity (conclusion [3], above) on the expected ionized masses.

We thank Drs. M. Mountain, M. Selby, S. Leggett, and Mr. M. Bird for assistance in obtaining the H_2 image of the Ring nebula at UKIRT and Drs. M. Smith, T. Geballe, and A. Longmore for measuring the CVF spectra. Mr. B. McNally and Mr. K. Krisciunas helped with production and calibration of the H_2 maps. We are grateful to Drs. R. Probst and R. Joyce for helping to obtain the K image of the Ring nebula and to E. Anderson for processing it. We profited from useful discussions

with L. H. Aller, G. Clark, A. Dalgarno, M. Greenhouse, J. P. Harrington, C. F. McKee, M. Morris, and J. M. Shull and especially M. Jura and B. Balick. Dr. G. R. Knapp kindly measured CO toward the Dumbbell nebula with the BTL 7 m telescope, at our request. Dr. J. B. Kaler supplied us with his up-to-date listing of optical line intensities for many of the PN in Table 6. The optical images supplied by Bruce Balick were processed at the University of Washington's Astronomical Image Processor, which was supported by the National Science Foundation Grant AST 83-10552. We thank Mr. R. L. O'Daniel for editing and typing the manuscript. This research was supported in part by NSF grant AST 83-18342 to UCLA. The UKIRT observations were made while Ian Gatley was a member of the staff of the United Kingdom Infrared Telescope Unit of the Royal Observatory, Edinburgh.

REFERENCES

Abt, H. A., and Levy, S. G. 1976, *Ap. J. Suppl.*, **30**, 273.
Alcock, C., and Ross, R. R. 1986, *Ap. J.*, **305**, 838.
Aller, L. H. 1986, private communication.
Aller, L. H., and Czyzak, S. J. 1979, *Ap. Space Sci.*, **62**, 397.
Atherton, P. D., Hicks, T. R., Reay, N. K., Robinson, G. J., Worswick, S. P., and Phillips, J. P. 1979, *Ap. J.*, **232**, 786.
Atherton, P. D., Hicks, T. R., Reay, N. K., Worswick, S. P., and Hayden Smith, W. 1978, *Astr. Ap.*, **66**, 297.
Balick, B. 1986, private communication.
———. 1987, *A.J.*, **94**, 671.
Beckwith, S., Beck, S. G., and Gatley, I. 1984, *Ap. J.*, **280**, 648.
Beckwith, S., Neugebauer, G., Becklin, E. E., and Mathews, K. 1980, *A.J.*, **85**, 886.
Beckwith, S., Persson, S. E., and Gatley, I. 1978, *Ap. J. (Letters)*, **219**, L33.
Black, J. H. 1978, *Ap. J.*, **222**, 125.
Black, J. H., and Dalgarno, A. 1976, *Ap. J.*, **203**, 132.
Black, J. H., Porter, A., and Dalgarno, A. 1981, *Ap. J.*, **249**, 138.
Calvert, N., and Peimbert, M. 1983, *Rev. Mexicana Astr. Ap.*, **5**, 319.
Capriotti, E. R., Cromwell, R. H., and Williams, R. E. 1971, *Ap. Letters*, **7**, 241.
Cerutti-Sola, M., and Perinotto, M. 1985, *Ap. J.*, **291**, 237.
Chernoff, D. F., Hollenbach, D. J., and McKee, C. F. 1982, *Ap. J. (Letters)*, **259**, L97.
Chu, Y. H., Jacoby, G. H., and Arendt, R. 1987, *Ap. J. Suppl.*, **64**, 529.
Cohen, M., and Barlow, M. J., 1975, *Ap. Letters*, **16**, 165.
Dalgarno, A. 1987, private communication.
Daub, C. T. 1982, *Ap. J.*, **260**, 612.
Draine, B. T., and Roberge, W. G. 1982, *Ap. J. (Letters)*, **259**, L91.
Duncan, J. C. 1937, *Ap. J.*, **86**, 496.
Gatley, I., *et al.* 1987, *Ap. J. (Letters)*, **318**, L73.
Gatley, I., and Kaifu, N. 1986, *IAU Symposium 120, Astrochemistry*, ed. M. S. Vardya and S. P. Tarafdar (Dordrecht: Reidel), p. 153.
Geballe, T. 1986, private communication.
Giuliani, J. L. 1981, *Ap. J.*, **245**, 903.
Goad, L. E. 1975, Ph.D. thesis, Harvard University.
Harrington, J. P. 1983, in *IAU Symposium 103, Planetary Nebulae*, ed. D. R. Flower (Dordrecht: Reidel), p. 219.
Harrington, J. P., and Feibelman, W. A. 1984, *Ap. J.*, **277**, 716.
Hawley, S. A., and Miller, J. S. 1977, *Ap. J.*, **212**, 94.
Heidner, R. F., and Kasper, V. V. 1972, *Chem. Phys. Letters*, **15**, 179.
Hippelein, H. H., Baessgen, M., and Grewing, M. 1985, *Astr. Ap.*, **152**, 213.
Hollenbach, D. J., and McKee, C. F. 1980, *Ap. J. (Letters)*, **241**, L47.
Hollenbach, D. J., Werner, M. W., and Salpeter, E. E. 1971, *Ap. J.*, **163**, 165.
Huggins, P. J. 1986, private communication.
Huggins, P. J., and Healy, A. P. 1986a, *Ap. J. (Letters)*, **305**, L29.
———. 1986*b*, *M.N.R.A.S.*, **220**, 33P.
Iben, I., and Renzini, A. 1983, *Ann. Rev. Astr. Ap.*, **21**, 271.
Isaacman, R. 1984, *Astr. Ap.*, **130**, 151.
Jewitt, D. C., Danielson, G. E., and Kupferman, P. N. 1986, *Ap. J.*, **302**, 727 (JDK).
Jura, M. 1983, *Ap. J.*, **275**, 683.
———. 1984*a*, *Ap. J.*, **282**, 200.
Jura, M. 1984*b*, *Ap. J.*, **286**, 630.
———. 1986*a*, *Ap. J.*, **309**, 732.
———. 1986*b*, *Irish Astr. J.*, **17**, 322.
Kahn, F. 1983, in *IAU Symposium 103, Planetary Nebulae*, ed. D. R. Flower (Dordrecht: Reidel), p. 305.
Kaler, J. B. 1976, *Ap. J. Suppl.*, **31**, 517.
———. 1983, *Ap. J.*, **271**, 188.
———. 1985, *Ann. Rev. Astr. Ap.*, **23**, 89.
———. 1986, private communication.
Khromov, G. S., and Kohoutek, L. 1968, *Bull. Astr. Inst. Czechoslovakia*, **19**, 1.
Knapp, G. R. 1985, in *Mass Loss From Red Giants*, ed. M. Morris and B. Zuckerman (Dordrecht: Reidel), p. 171.
———. 1986, private communication.
Kwok, S. 1983, in *IAU Symposium 103, Planetary Nebulae*, ed. D. R. Flower (Dordrecht: Reidel), p. 293.
———. 1985, *Ap. J.*, **290**, 568.
Lepp, S., and Shull, J. M. 1983, *Ap. J.*, **270**, 578.
Likkel, L., Omont, A., Morris, M., and Forveille, T. 1987, *Astr. Ap.*, **173**, L11.
Livio, M., Salzman, J., and Shaviv, G. 1979, *M.N.R.A.S.*, **188**, 1.
Morris, M. 1981, *Ap. J.*, **249**, 572.
———. 1985, in *Mass Loss From Red Giants*, ed. M. Morris and B. Zuckerman (Dordrecht: Reidel), p. 129.
Peimbert, M., and Torres-Peimbert, S. 1983, in *IAU Symposium 103, Planetary Nebulae*, ed. D. R. Flower (Dordrecht: Reidel), p. 233.
Persson, S. E., McGregor, P. J., Duncan, D. K., Lanning, H., and Geballe, T., and Lonsdale, C. 1984, in *XVI ESLAB Symposium* (ESA Document SP 192) (Nordwijk: ESA), p. 41.
Phillips, J. P., and Reay, N. K. 1977, *Astr. Ap.*, **59**, 91.
Pottasch, S. 1980, *Astr. Ap.*, **89**, 336.
Reid, M. J., *et al.* 1979, *Ap. J. (Letters)*, **227**, L89.
Roberge, W., and Dalgarno, A. 1982, *Ap. J.*, **255**, 176.
Schaefer, B. E. 1985, *Ap. J.*, **297**, 245.
Schmidt, G. D., and Cohen, M. 1981, *Ap. J.*, **246**, 444.
Shull, J. M., and Beckwith, S. 1982, *Ann. Rev. Astr. Ap.*, **20**, 163.
Storey, J. W. V. 1984, *M.N.R.A.S.*, **206**, 521.
Taylor, A. R., and Pottasch, S. R. 1987, *Astr. Ap.*, **176**, L5.
Torres-Peimbert, S., and Peimbert, M. 1977, *Rev. Mexicana Astr. Ap.*, **2**, 181.
Tylenda, R. 1986, *Astr. Ap.*, **156**, 217.
van der Veen, W., Habing, H. J., and Geballe, T. 1987, in *Planetary and Proto-Planetary Nebulae: From IRAS to ISO*, ed. A. Preite-Martinez (Dordrecht: Reidel), in press.
Wilson, O. C. 1958, *Rev. Mod. Phys.*, **30**, 1025.
Wood, P. R., and Faulkner, D. J. 1986, *Ap. J.*, **307**, 659.
Wright, A. E., and Barlow, M. J. 1975, *M.N.R.A.S.*, **170**, 41.
Zuckerman, B. 1980, *Ann. Rev. Astr. Ap.*, **18**, 263.
Zuckerman, B., and Aller, J. H. 1986, *Ap. J.*, **301**, 772 (ZA).
Zuckerman, B., and Dyck, H. M. 1986, *Ap. J.*, **304**, 394.
———. 1987, *Astr. Ap.*, submitted.
Zuckerman, B., Dyck, H. M., and Claussen, M. 1986, *Ap. J.*, **304**, 401.
Zuckerman, B., and Lo, K. Y. 1987, *Astr. Ap.*, **173**, 263.
Zuckerman, B., Terzian, Y., and Silverglate, P. 1980, *Ap. J.*, **241**, 1014.

IAN GATLEY: NOAO, 950 North Cherry Avenue, Tucson, AZ 85726

BENJAMIN M. ZUCKERMAN: UCLA, 405 Hilgard Avenue, Los Angeles, CA 90024